Inorganic Chemistry

Article

pubs.acs.org/IC

# Activation of Nitrogen Brønsted Acids: Synthesis and Reactivity of a New Class of Nitrogen Acid Complexes

D. Scott Bohle* and Zhijie Chua

Department of Chemistry, McGill University, 801 Sherbrooke Street. W., Montreal, Quebec H3A 0B8, Canada

Supporting Information

**ABSTRACT:** The nitrogen acids $RC(O)NHNO_2$, N-nitroamide, R = $CH_3$ (**1**), $C_2H_5$ (**2**) and N-nitrocarbamate, $R'OC(O)NHNO_2$, R′ = $CH_3$ (**3**), $C_2H_5$ (**4**) are a class of primary N-nitrocarboxamide compounds that oxidatively add to *trans*-$Ir^{(I)}(Cl)(N_2)(PPh_3)_2$ to give six-coordinate $Ir^{(III)}(\eta^2\text{-}(NO_2)$-nitrogen acid)$(H)(Cl)(PPh_3)_2$ complexes **5**–**8**. Unexpected fluxional behavior of the complexes in solution is observed by $^1H$ NMR spectroscopy. Reaction intermediates of the oxidative addition reactions were also observed and monitored using $^{31}P$ and $^1H$ NMR and solution IR spectroscopies. Complex **5** reacts with methyl triflate in $CH_3CN$ to generate bis(acetonitrile) complex (**9**) from a net loss of the nitrogen acid anion. $P(CH_3)_2Ph$ reacts with **5** to give phosphine-substituted and $P(CH_3)_2Ph$ addition isomers (**10**). Reactivity studies of **5** with CO gave metastable CO adduct isomer **11**, which loses CO on prolonged standing in solution.

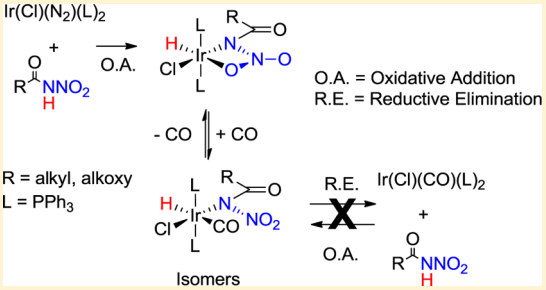


## INTRODUCTION

The organometallic chemistry of the carbon acids is now well-developed with CH oxidative addition being a universal reaction for this species.[1] In contrast, the corresponding class of nitrogen acids has a much less-developed organometallic chemistry, with only a handful of N–H oxidative addition reactions being recognized.[2] Although many nitrogen compounds can coordinate to transition metal complexes as simple Lewis base ligands, in certain cases they can oxidatively add (Scheme 1). Electron-withdrawing substitutents R favor the latter pathway.

**Scheme 1. Carbon and Nitrogen Acids**

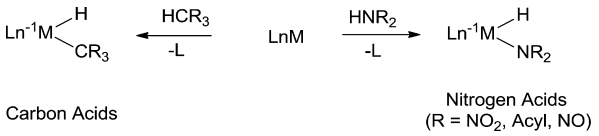


In prior work, we have established the activation product of N-nitropropionamide (**2**) with *trans*-$Ir(Cl)(N_2)(PPh_3)_2$ to give a nitrogen chelate with an unusual O-bound nitro group.[3] However, the full spectroscopic evaluation and reactivity of this class of complexes were not examined. In this paper we describe (1) the synthesis of the ligands, (2) the synthesis of the nitrogen acid ligand complexes using *trans*-$Ir(Cl)(N_2)(PPh_3)_2$, (3) dynamic process of the complexes in solution, (4) observed reaction transient intermediates, and (5) reactivity studies of $Ir(CH_3C(O)NNO_2)(H)(Cl)(PPh_3)_2$ (**5**). Taken together these results demonstrate that the N-nitroamides/carbamates are good $\pi$-acceptor ligands that are readily introduced into low-valent transition metals by oxidative addition.

## EXPERIMENTAL SECTION

**General Experimental.** Except where noted all reagents and solvents are used as supplied commercially. Methanol is dried by distillation from freshly generated magnesium methoxide, and dry hexane is distilled from sodium benzophenone ketyl. $^1H$ NMR spectra are recorded on Varian Mercury 200, 400, or 500 MHz spectrometers, and $^{13}C$ NMR spectra are recorded on a Varian Mercury 300 MHz spectrometer. All chemical shifts are recorded in $\delta$ (ppm) relative to residual solvent signals for $^1H$ and $^{13}C$ spectra. Melting/decomposition points are measured by using a TA-Q2000 differential scanning calorimeter calibrated against an internal standard. The IR spectra are recorded in KBr disks for solution, KBr matrix for solids, or a gastight cell for gas-phase spectra by using ABB Bomem MB Series IR spectrometer with spectral resolution of 2 $cm^{-1}$. Elemental analyses are performed in the Elemental Analyses Laboratory at University of Montreal. Sublimation purifications are carried out under vacuum with cold-finger inserts containing dry ice–acetone mixtures or ice–water and heated to the required temperatures. Nitramide is synthesized from literature methods with modification.[4] N-nitropropionamide (**2**) and $Ir(\eta^2\text{-}C_2H_5C(O)NNO_2)(H)(Cl)(PPh_3)_2$ (**6**) has been reported previously.[3] Additional spectroscopic characterization of the transient intermediates can be found in the Supporting Information.

**X-ray Crystallography.** Crystals are mounted on glass fibers with epoxy resin or Mitegen mounts using Paratone-N from Hampton Research, and single-crystal X-ray diffraction experiments are carried out with a BRUKER SMART CCD or BRUKER APEX-II CCD diffractometer by using graphite-monochromated Mo K$\alpha$ radiation ($\lambda$ = 0.710 73 Å) and KRYOFLEX for low-temperature experiments. SAINT[5] is used for integration of the intensity reflections and scaling,

**Received:** July 22, 2014
**Published:** October 3, 2014

   dx.doi.org/10.1021/ic5017033 | *Inorg. Chem.* 2014, 53, 11160–11172

and SADABS[6] is used for absorption correction. Direct methods are used for structures that do not contain heavy atoms or show pseudomerohedral twinning, corrected using PLATON,[7], while Patterson maps are used for the rest of the structures to generate the initial solution. Non-hydrogen atoms are located by difference Fourier maps, and final solution refinements are solved by full-matrix least-squares method on $F^2$ of all data, by using SHELXTL[5] software. The hydrogen atoms are placed in calculated positions.

Crystals of **1**−**4** are grown from slow evaporation of $CH_2Cl_2$ at room temperature, while those of **5**−**8** are grown from $CH_2Cl_2$/$CH_3OH$ layered solutions at −21 °C, and those of **10** are from MeCN/ether layered solutions. Crystallographic data and data-collection parameters for the nitrogen acids and Ir(III) complexes are shown in Supporting Information, Table S1.

**Theoretical Calculations.** Density functional theory (DFT) calculations are performed with the Gaussian03 program with the B3LYP functionals and 6-311++g** basis sets. The Z and E ground-state structures correspond to local minima with all-positive vibrational modes; the transition states, located by the quadratic synchronous transit algorithm, are then checked with an intrinsic reaction coordinate(IRC) analysis following calculations to ensure that the transition state corresponds to the E and Z isomerization.

**Synthesis of N-Nitroacetamide[8] $CH_3C(O)NHNO_2$ (1).** A modified literature preparation of *N*-nitroacetamide[4b] was devised. Briefly, nitramide (0.500 g, 8.06 mmol) is dissolved in ether (5 mL) and cooled to 0 °C in an ice-bath. Acetic anhydride (10 mL, 105.8 mmol) is then added followed by LiCl (0.4 mg, 9.41 $\mu$mol), and the reaction mixture is allowed to warm to room temperature. The reaction mixture is stirred for 24 h and subjected to vacuum evaporation at $T$ < 40 °C to give white solids, which are purified by vacuum sublimation (dry ice−acetone) at 70 °C to give colorless crystals of *N*-nitroacetamide (**1**) (0.350 g, 3.37 mmol, 42% yield). IR (KBr, $cm^{-1}$): 3433w, 3252m, 3156s, 3018s, 2856m, 2811m, 2735w, 2570w, 1962w, 1728vs, 1623vs, 1443s, 1309vs, 1196vs, 1016vs, 1007vs, 952m, 764m, 723m, 605s, 569m, 454w. Gas-phase IR ($cm^{-1}$): 1747s, 1738s, 1732s, 1623vs, 1430m, 1371s, 1316s, 1230s, 1185s, 1011m. Raman ($cm^{-1}$): 2952vw, 1718m, 1638w, 1307m, 1194m, 1005m, 954m, 763m, 608vs, 454m, 389m, 246w. $^1$H NMR (200 MHz, $CDCl_3$) ppm: $\delta$ = 2.52 (s, $CH_3$), 10.52 (N*H*, broad). $^{13}$C NMR (75 MHz, $CDCl_3$) ppm: $\delta$ = 24.13 (s), 168.08 (s).

**Synthesis of N-Nitromethylcarbamate[9] $CH_3OC(O)NHNO_2$ (3).** Methyl carbamate (1.000 g, 13.3 mmol) is gradually added at 25 °C to a mixture of concentrated $H_2SO_4$ (15 mL) and $KNO_3$ (2.03 g, 20.01 mmol). The mixture is stirred for 15 min at 25 °C, poured onto crushed ice (14.2 g) with stirring, and extracted with ether (7 × 6 mL). The ether extracts are dried with anhydrous $MgSO_4$, and the solvent is removed in vacuo to dryness. The white solids are redissolved in ether (20 mL), and $NH_3$ is bubbled into the mixture in an ice−water bath to give a white precipitate. The white precipitate is filtered, dried, and collected to give ammonium N-nitromethylcarbamate ($\mathbf{3NH_4}$)[10] (1.682 g, 12.3 mmol, 92% yield).

Compound $\mathbf{3NH_4}$ (1.682 g, 12.3 mmol) is gradually dissolved in $H_2SO_4$ (1 mL of concentrated $H_2SO_4$, 3.0 g of ice, and 10 mL of deionized $H_2O$) and stirred until the mixture is homogeneous. The solution is extracted with ethyl acetate (7 × 10 mL), and the extracts are dried over anhydrous $MgSO_4$. The solvent is removed in vacuo, and the white residue is purified by vacuum sublimation (dry ice−acetone) at 65−70 °C to give N-nitromethylcarbamate (**3**) (1.230 g, 10.3 mmol, 77% yield). mp: 91.0 °C (8.65 kJ $mol^{-1}$). IR (KBr, $cm^{-1}$): 3245s, 3206s, 3060w, 3024w, 2972w, 2850vw, 1748vs, 1615vs, 1549w, 1458s, 1414m, 1325m, 1244s, 1092w, 1003m, 947m, 771m, 736,w, 625m, 456w. $^1$H NMR (200 MHz, $CDCl_3$) ppm: $\delta$ = 3.91 (s, $CH_3$), 10.12 (s, broad, N*H*).

**Synthesis of N-Nitroethylcarbamate[11] $C_2H_5OC(O)NHNO_2$ (4).** This preparation is a combination of separate methods for the synthesis of the ammonium salt and the free base of the nitrogen acid with modifications. Ethyl carbamate (1.000 g, 11.2 mmol) is gradually added at temperature less than 25 °C to a mixture of concentrated $H_2SO_4$ (15 mL) and $KNO_3$ (2.03 g, 20.01 mmol). The mixture is stirred for 15 min at 25 °C, poured onto crushed ice (12 g) with stirring, and extracted with $CH_2Cl_2$ (7 × 45 mL). The $CH_2Cl_2$ extracts are dried with anhydrous $MgSO_4$, and the solvent is removed in vacuo until dryness. The white solids are redissolved in ether (20 mL), and $NH_3$ is bubbled into the mixture for 2 min in an ice−water bath to give a white precipitate. The white precipitate is filtered, dried, and collected to give ammonium N-nitroethylcarbamate ($\mathbf{4NH_4}$)[10] (1.607 g, 10.64 mmol, 95% yield).

Compound $\mathbf{4NH_4}$ (1.607 g, 10.64 mmol) is gradually dissolved in $H_2SO_4$ (1 mL of concentrated $H_2SO_4$, 3.0 g of ice, and 10 mL of deionized $H_2O$) and stirred until homogeneous. The solution is extracted with ethyl acetate (7 × 10 mL), and the extracts are dried over anhydrous $MgSO_4$. The solvent is removed in vacuo, and the white residue is purified by vacuum sublimation (dry ice−acetone) at 65−70 °C to give *N*-nitroethylcarbamate (**4**) (1.244 g, 9.21 mmol, 87% yield). Complete spectroscopic data for this preparation follows and matches the limited literature data. mp: 67.7 °C (14.5 kJ $mol^{-1}$). IR (KBr, $cm^{-1}$): 3235s, 3007m, 2988m, 2947w, 2880w, 2810w, 1741vs, 1605vs, 1548m, 1518m, 1453s, 1391s, 1368m, 1329s, 1227s, 1116m, 1017m, 997m, 878m, 798m, 768m, 731w, 603m, 458w. $^1$H NMR (200 MHz, $CDCl_3$) ppm: $\delta$ = 1.36 (t, $CH_3$, $J$ = 7.1 Hz), 4.36 (q, $CH_2$, $J$, = 7.1 Hz), 9.90 (s, broad, N*H*).

**Synthesis of Ir($\eta^2$-$CH_3C(O)NNO_2$)(H)(Cl)($PPh_3$)$_2$ (5).** *trans*-Ir(Cl)($N_2$)($PPh_3$)$_2$ (0.110 g, 0.141 mmol), **1** (0.020 g, 0.192 mmol), and degassed $CHCl_3$ (5 mL) are mixed and stirred under a $N_2$ atmosphere. Gas evolution is observed, and the reaction mixture is stirred for 3 h. The reaction mixture is dried in vacuo to give a yellow residue, which is recrystallized from $CH_2Cl_2$/$CH_3OH$ to give yellow crystals of Ir($\eta^2$-$CH_3C(O)NNO_2$)(H)(Cl)($PPh_3$)$_2$ (**5**) (0.104 g, 0.121 mmol, 86% yield). IR ($cm^{-1}$): 3056w, 2963vw, 2322vw, 2068vw, 1696m, 1572vw, 1514s, 1483m, 1435s, 1363w, 1261w, 1241w, 1198s, 1096s, 1035m, 806m, 745m, 707m, 695vs, 621w, 520vs, 504m. Raman ($cm^{-1}$): 3067vw, 2326w, 1590m, 1190w, 1098m, 1030m, 1002vs, 891w, 704m, 617m, 542w, 255m. $^1$H NMR (200 MHz, $CDCl_3$) ppm: $\delta$ = −31.78 (s, Ir-*H*, broad), 1.23 (s, $CH_3$), 7.38 (m, 18H-$PPh_3$), 7.62 (m, 12H-$PPh_3$). $^1$H NMR (400 MHz, $CDCl_3$) ppm: $\delta$ = −31.74 (s, Ir-*H*, broad), 1.25 (s, $CH_3$). $^1$H NMR (200 MHz, $C_6D_6$) ppm: $\delta$ = −31.22 (t, Ir-*H*, $J_{P-H}$ = 13.4 Hz), 1.47 (s, $CH_3$), 6.92 (m, 18H-$PPh_3$), 7.88 (m, 12H-$PPh_3$). $^1$H NMR (400 MHz, $C_6D_6$) ppm: $\delta$ = −31.22 (s, Ir-*H*, broad), 1.48 (s, $CH_3$). $^{31}$P NMR (81 MHz, $CDCl_3$) ppm: $\delta$ = 11.42 (s). $^{31}$P NMR (81 MHz, $C_6D_6$) ppm: $\delta$ = 10.92 (s). Electrospray ionization mass spectrometry (ESI-MS): 878.92 $[M + Na]^+$. Anal. Calcd for $C_{38}H_{34}N_2O_3P_2ClIr{\cdot}CH_2Cl_2$ (941.24 g $mol^{-1}$) % C, 49.72; H, 3.82; N, 2.97. Found % C, 49.22; H: 3.74; N, 2.85.

**Synthesis of Ir($\eta^2$-$CH_3OC(O)NNO_2$)(H)(Cl)($PPh_3$)$_2$ (7).** *trans*-Ir(Cl)($N_2$)($PPh_3$)$_2$ (0.015 g, 0.0192 mmol), **3** (0.003 g, 0.002 mmol), and degassed $CHCl_3$ (3 mL) are mixed and stirred under a $N_2$ atmosphere. Gas evolution is observed, and the reaction mixture is stirred for 3 h. The reaction mixture is evacuated in vacuo to give yellow solids, which are recrystallized from $CH_2Cl_2$/$CH_3OH$ to give yellow crystals of Ir($\eta^2$-$CH_3OC(O)NNO_2$)(H)(Cl)($PPh_3$)$_2$ (**7**) (0.012 g, 0.0133 mmol, 69% yield). IR (KBr, $cm^{-1}$): 3056w, 2953vw, 2920vw, 2850vw, 2298vw, 1747s, 1518m, 1483m, 1434s, 1266m, 1212m, 1185m, 1161w, 1097s, 1028w, 998w, 843w, 795w, 747m, 695s, 918vw, 520vs, 503m, 462w. $^1$H NMR (200 MHz, $CDCl_3$) ppm: $\delta$ = −31.69 (t, Ir−H, $J_{P-H}$ = 13.2 Hz), 2.97 (s, $CH_3$), 7.34 (m, 18H-$PPh_3$), 7.62 (m, 12H-$PPh_3$). $^{31}$P NMR (81 MHz, $CDCl_3$) ppm: $\delta$ = 9.97 (s) but the $^1$H coupled spectrum is a exchange broadened doublet ($J_{P-H}$ = 4.5 Hz Hz). Anal. Calcd for $C_{38}H_{34}N_2O_4P_2ClIr{\cdot}CH_2Cl_2$ (957.23 g $mol^{-1}$) % C, 48.89; H, 3.76; N, 2.93. Found % C, 49.11; H, 3.62; N, 2.85.

**Synthesis of Ir($\eta^2$-$C_2H_5OC(O)NNO_2$)(H)(Cl)($PPh_3$)$_2$ (8).** *trans*-Ir(Cl)($N_2$)($PPh_3$)$_2$ (0.010 g, 0.100 mmol), **4** (0.014 g, 0.104 mmol), and degassed $CHCl_3$ (5 mL) are mixed and stirred under a $N_2$ atmosphere. Gas evolution is observed, and the reaction mixture is stirred for 3 h. The reaction mixture is evacuated to give yellow residues, which are recrystallized from $CH_2Cl_2$/hexanes to give yellow crystals of Ir($\eta^2$-$C_2H_5OC(O)NNO_2$)(H)(Cl)($PPh_3$)$_2$ (**8**) (0.053 g, 0.060 mmol, 60% yield). IR (KBr, $cm^{-1}$): 3056w, 2988vw, 2923vw, 1747m, 1517m, 1483m, 1435s, 1207s, 1095vs, 1028m, 999w, 745m, 695vs, 542m, 522vs $^1$H NMR (200 MHz, $CDCl_3$) ppm: $\delta$ = −31.80 (t,


dx.doi.org/10.1021/ic5017033 | *Inorg. Chem.* 2014, 53, 11160−11172

Ir-*H*, $J_{P-H}$ = 13.6 Hz), 0.88 (t, $CH_3$, $J$ = 7.2 Hz), 3.32 (q, $CH_2$, $J$ = 7.2 Hz), 7.40 (m, 18H-$PPh_3$), 7.64 (m, 12H-$PPh_3$). $^1$H NMR (400 MHz, $CDCl_3$) ppm: $\delta$ = −31.81 (t, Ir-*H*, $J_{P-H}$ = 14 Hz), 0.87 (t, $CH_3$, $J$ = 8 Hz), 3.32 (q, $CH_2$, $J$ = 8 Hz), 7.39 (m, 18H-$PPh_3$), 7.65 (m, 12H-$PPh_3$). $^1$H NMR (200 MHz, $C_6D_6$) ppm: $\delta$ = −30.88 (t, Ir-*H*, $J_{P-H}$ = 13.5 Hz), 0.61 (t, $CH_3$, $J$ = 7.2 Hz), 3.23 (q, $CH_2$, $J$ = 7.2 Hz), 6.96 (m, 18H-$PPh_3$), 7.87 (m, 12H-$PPh_3$). $^1$H NMR (400 MHz, $C_6D_6$) ppm: $\delta$ = −30.91 (t, Ir-*H*, $J_{P-H}$ = 12 Hz), 0.61 (t, $CH_3$, $J$ = 8 Hz), 3.23 (q, $CH_2$, $J$ = 8 Hz), 6.96 (m, 18H-$PPh_3$), 7.87 (m, 12H-$PPh_3$). $^{31}$P NMR (81 MHz, $CDCl_3$) ppm: $\delta$ = 10.35 (s). $^{31}$P NMR (81 MHz, $C_6D_6$) ppm: $\delta$ = 10.71 (s). ESI-MS: 884.96 $[M - H]^+$. Anal. Calcd for $C_{39}H_{36}N_2O_4P_2ClIr{\cdot}0.3C_6H_{14}$ (912.19 g mol$^{-1}$) % C, 53.72; H, 4.44; N, 3.07. Found % C, 53.30; H, 4.82; N, 2.58.

**General Procedure for Solution IR Reaction Monitoring.** In a typical experiment, *trans*-Ir(Cl)($N_2$)($PPh_3$)$_2$ (0.010 g, 0.013 mmol) and nitrogen acid (slight excess of 0.013 mmol) are charged into a reaction flask under a $N_2$ atmosphere. Cooled degassed $CHCl_3$ (5 mL) is added, and the reaction is monitored at −10 °C, during which time, aliquots are removed for IR analysis and returned.

**Reaction of 5 with Methyl Trifluoromethanesulfonate.** Complex **5** (0.050 g, 0.058 mmol) is dissolved in dry $CH_3CN$ (4 mL) under a $N_2$ atmosphere. Methyl trifluoromethanesulfonate (7 $\mu$L, 0.064 mmol) is added and stirred for 2 h. The reaction mixture is observed to change from pale yellow to colorless. The solvent is removed in vacuo to give tan solids, which are recrystallized from $CH_3CN$/ether to give $[Ir(H)(Cl)(CH_3CN)_2(PPh_3)_2][SO_3CF_3]$ (**9**) (18 mg, 0.022 mmol, 37% yield). IR (KBr, cm$^{-1}$): 3059w, 3024vw, 3005vw, 2990vs, 2931vw, 2296vw, 2272vw, 2251vw, 1483m, 1435s, 1270vs, 1224m, 1187m, 1154m, 1096m, 1031s, 999m, 753m, 709m, 695s, 638s, 524vs, 504m. $^1$H NMR (200 MHz, $CDCl_3$) ppm: −20.67 (t, Ir-*H*, $J_{P-H}$ = 12.3 Hz), 1.91 (s, 3H), 2.00 (s, 3H), 7.46 (m. $PPh_3$), 7.69 (m, $PPh_3$). $^{31}$P NMR (81 MHz, $CDCl_3$) ppm: 4.43 (s). ESI-MS: 793.81 $[M - CH_3CN]^+$.

**Reaction of 5 with $P(CH_3)_2Ph$.** Complex **5** (0.060 g, 0.070 mmol) is dissolved in dry $CHCl_3$ (5 mL). $P(CH_3)_2Ph$ (21 $\mu$L, 0.147 mmol) is added and stirred for 3 h. The solution turned slightly pale yellow over time, and the solvent was removed in vacuo. The oil that remained contains Ir($\eta^2$-$CH_3C(O)NNO_2$)(H)(Cl)($P(CH_3)_2Ph$)$_2$ (**10A**) and isomers of Ir($\eta^1$-$CH_3C(O)NNO_2$)(H)(Cl)($P(CH_3)_2Ph$)$_3$ (**10B**−**10D**) in ratio of 0.18:0.42:0.10:0.30, respectively (approximately 0.043 g). $^1$H NMR (200 MHz, $CDCl_3$) ppm: (**10C**) −21.48 (dt, Ir-*H*, $J_{cis\ P-H}$ = 19.2 Hz, $J_{cis\ P-H}$ = 12.2 Hz, fraction of minor isomer = 0.10), (**10B**) −19.96 (dt, Ir-*H*, $J_{cis\ P-H}$ = 19.8 Hz, $J_{cis\ P-H}$ = 12.2 Hz, fraction of major isomer = 0.42), (**10A**) −19.68 (t, Ir-*H*, $J_{P-H}$ = 13.2 Hz fraction of minor isomer = 0.18), (**10D**) −11.63 (dt, Ir-*H*, $J_{trans\ P-H}$ = 157.8 Hz, $J_{cis\ P-H}$ = 16.0 Hz, fraction of minor isomer = 0.30). $^{31}$P NMR (81 MHz, $CDCl_3$) ppm: −44.37 (s, free $P(CH_3)_2Ph$), fraction of combined three isomers (**10B**−**10D**) = 0.82; −34.56 (t, $P(CH_3)_2Ph$, $J_{cis\ P\text{-}trans\ P}$ = 19.9 Hz), −20.12 (d, $PPh_3$, $J_{trans\ P\text{-}cis\ P}$ = 19.9 Hz), −4.38 (s, free $PPh_3$), (**10A**) 35.13 (s, minor isomer = 0.18).

**Reaction of 5 with CO.** Complex **5** (0.030 g, 0.035 mmol) is dissolved in $CHCl_3$ (5 mL). CO is vigorously bubbled into the solution. The yellow solution turned pale yellow after 10 min. The solvent is removed in vacuo, and the pale yellow solids recrystallized from $CH_2Cl_2$/hexanes to give pale yellow solids that contain isomers (0.05:0.56:0.39) of Ir($\eta^1$-$CH_3C(O)NNO_2$)(H)(Cl)(CO)($PPh_3$)$_2$ (**11**) (0.030 mg, 0.034 mmol, 97% yield). IR (cm$^{-1}$): 3056w, 2962vw, 2185vw (broad), 2047m (CO), 1695vw, 1648vw (broad), 1511m, 1483m, 1435s, 1362w, 1262w, 1188m, 1095s, 1029m, 1000m, 745m, 694vs, 524vs $^1$H NMR (400 MHz, $CDCl_3$) ppm: $\delta$ = −8.31 (t, Ir-*H*, $J_{P-H}$ = 16 Hz, minor isomer = 0.05), −7.68 (t, Ir-*H*, $J_{P-H}$ = 12 MHz, major isomer = 0.56), −7.54 (t, Ir-*H*, $J_{P-H}$ = 12 MHz, minor isomer = 0.39), 1.15 (s, 3H, minor isomer = 0.41), 1.57 (s, 3H, major isomer = 0.59). $^{31}$P NMR (81 MHz, $CDCl_3$) ppm: $\delta$ = 3.61 (s, minor isomer = 0.43), 3.92 (s, major isomer = 0.57). Upon leaving the reaction mixture in solution overnight, **5** is regenerated, as confirmed by the loss of the 2047 cm$^{-1}$ band. $^{31}$P NMR shows only the appearance of a single resonance at 11.45 ppm (**5**). Repeated CO bubbling regenerated the three isomers of **11** again.

## RESULTS AND DISCUSSION

**Synthesis of N-Nitro Compounds.** Primary N-nitroamides synthesis have been described previously and are prepared by acylation of nitramide with acid anhydrides (Scheme 2a).[3] This contrasts with the synthesis of N-nitrocarbamates, where nitration of the corresponding primary alkylcarbamates with $KNO_3$ in concentrated $H_2SO_4$ is sufficient to give very good yields of the nitro compounds (Scheme 2b).

**Scheme 2. Synthesis of (a) N-Nitroamides and (b) N-Nitrocarbamates**

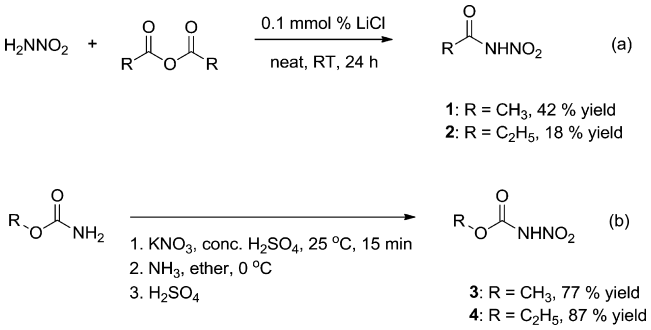


There is only limited spectroscopic information for primary N-nitroamides and N-nitrocarbamates except for **4**[11] with most of the prior studies concerning secondary N-nitrocarboxamides.[9b] There are some rare instances of limited IR characterization of the N-nitroamides.[8] There are, however, numerous data for the related nitramines $R_2NNO_2$, which have similar vibrational data to the N−$NO_2$ compounds reported here.

The primary N-nitroamides and N-nitrocarbamates have amidic protons that are observed between 9−11 ppm in $^1$H NMR. This chemical shift is similar to that of nitramide where the amide proton is observed between 8−11 ppm depending on solvent.[3,12] For simple nitramines,[13] the chemical shift effect on the $\alpha$-H of the −N($NO_2$) group is similar to that of alkoxy substituents.[14] The alkyl substituents of the N-nitroamides and N-nitrocarbamates are all observed slightly downfield (approximately 0.2 to 0.4 ppm difference) from the generic region of the regular amides and esters probably due to the inductive effect of the nitro group.

The N-nitroamides and N-nitrocarbamates also exhibit interesting IR bands (Figure 1). In particular, the presence of the acyl- and nitro-conjugated system gives rise to unique bands that do not reside in the usual ranges for the respective functional groups. Some suitable references that would help in the assignment of these vibrational bands include the regular amides,[15] carbamates,[15,16] and nitramines[14] (Figure 1).

For the N-nitroamides, a new strong band is observed between 1000−1100 cm$^{-1}$, which is assigned to a mode that is predominantly a N−N bond-stretching band. For the N-nitrocarbamates, several new bands are also observed around the 900 to 1150 cm$^{-1}$ region. These bands are assigned to the carbamate stretching modes. The lowest energy, strong absorption band in this region, 900−1000 cm$^{-1}$, has significant $\nu$(N−N) character. The IR bands of **4** match well with the literature assignment.[11]

**Synthesis of Ir(III) N-Nitrocarboxamides Complexes.** The amide proton of the N-nitro compounds **1**−**4** is acidic due to the electron-withdrawing nature of the nitro group, and these nitrogen acids oxidatively add to *trans*-Ir(Cl)($N_2$)($PPh_3$)$_2$ (Scheme 3).


dx.doi.org/10.1021/ic5017033 | Inorg. Chem. 2014, 53, 11160−11172

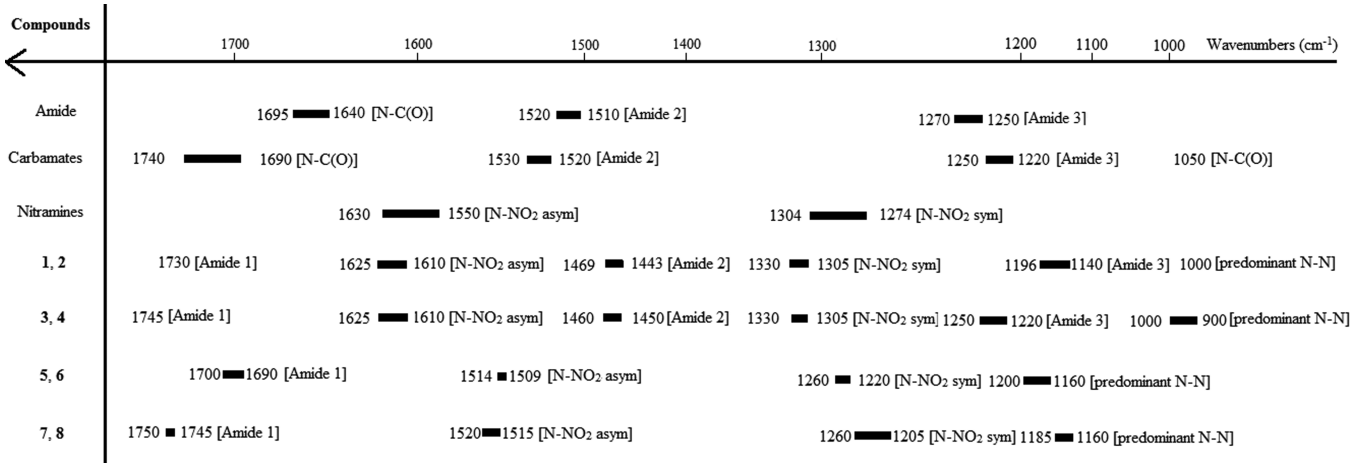


**Figure 1.** Infrared bands for primary N-nitroamides, N-nitrocarbamates, and related compounds.

**Scheme 3. Reaction of *trans*-Ir(Cl)($N_2$)($PPh_3$)$_2$ with Nitrogen Acids 1−4**

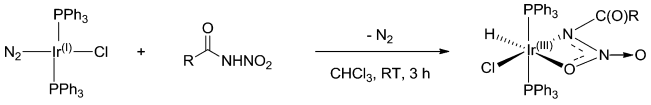


| R | Compound |
|---|---|
| $CH_3$ | **1** |
| $C_2H_5$ | **2** |
| $CH_3O$ | **3** |
| $C_2H_5O$ | **4** |

| R | Complex |
|---|---|
| $CH_3$ | **5** |
| $C_2H_5$ | **6** |
| $CH_3O$ | **7** |
| $C_2H_5O$ | **8** |

In all of the above reactions, vigorous evolution of gas was observed at the start of the reaction, which is most likely from the loss of $N_2$. The reaction mixture was stirred at room temperature over 3 h, during which time, the color turned from a deep yellow to pale yellow. Subsequent workup of the reaction mixtures gave good yields of the new Ir complexes **5**−**8**.

The $^{31}$P NMR spectroscopy of the Ir(III) complexes all show a single resonance signal, which corresponds to a single isomer in solution. The Ir hydride resonance is located between −30 to −40 ppm and appears as triplets for **6**, **7**, and **8** but is a broad signal for **5** in $CDCl_3$, which will be discussed below. The alkyl and alkoxy groups are also located downfield compared to the free acid.

The vibrational spectra of complexes **5**−**8** have unusual bands associated with the coordinated ligand. Of great interest is the weak $\nu$(Ir−H) band for **5**, **6**, and **7** at 2322, 2311, and 2298 cm$^{-1}$, respectively, while no such band is observed in **8**. A possible reason for the low intensity could be the Ir−H bond has little polarity, resulting in a small change in dipole moment. There is, however, a medium-intensity band observed around

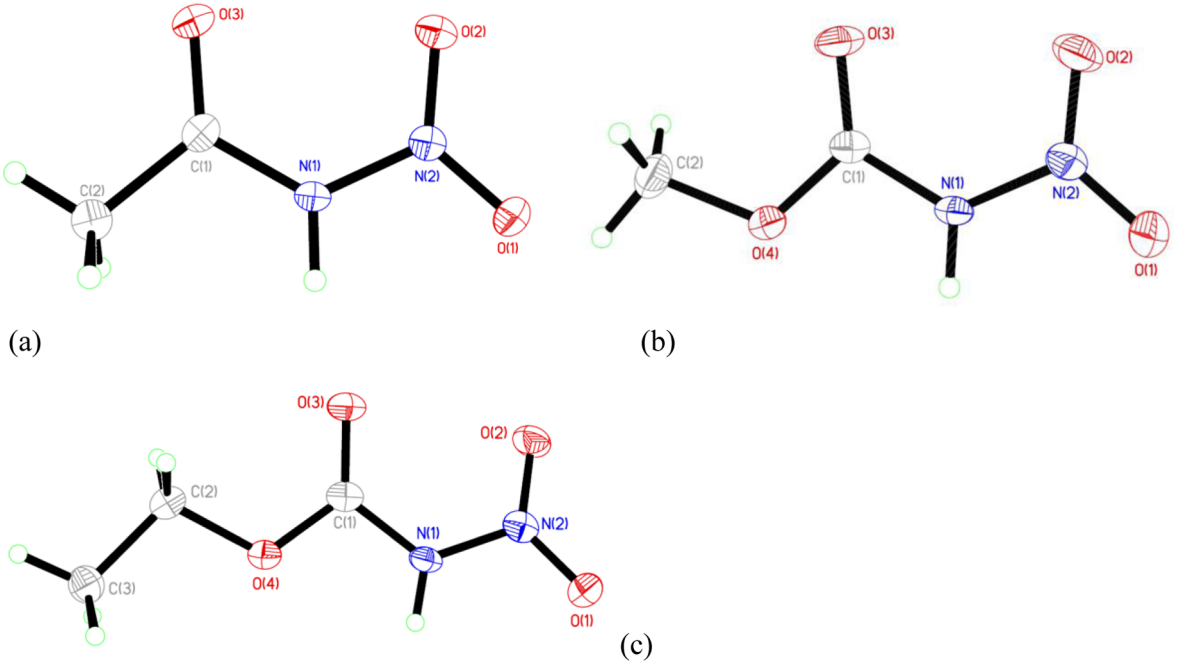


**Figure 2.** ORTEP plots of the nitrogen acids at 50% thermal ellipsoid. (a) *N*-nitroacetamide (**1**). (b) *N*-nitromethylcarbamate (**3**). (c) *N*-nitroethylcarbamate (**4**).


dx.doi.org/10.1021/ic5017033 | *Inorg. Chem.* 2014, 53, 11160−11172

805 $cm^{-1}$ in **5**–**7**, which can be assigned to the $\delta$(Ir–H) bending mode.[17] Other unique vibrational bands depicted in Figure 1 are roughly assigned to the functional groups in the coordinated conjugate base.

The successful reaction of *trans*-Ir(Cl)($N_2$)($PPh_3$)$_2$ with the nitrogen acids differs from that of Vaska's complex, *trans*-Ir(Cl)(CO)($PPh_3$)$_2$. With Vaska's complex, stoichiometric addition of **1** results in some formation of a new compound, as indicated in $^{31}$P and $^{1}$H NMR monitoring, but the reaction does not go to completion even under reflux conditions. Furthermore, increasing the stoichiometry of the nitrogen acid results in formation of complex mixtures. The implication for the above observations is that the reaction could be reversible or in equilibrium initially, but with excess **1** this leads to product inhibition due to the formation of small amounts of base derived from some decomposition of **1**. It has been established that the extent of oxidative addition of an acid to Vaska's complex is related to the strength of the acid (p$K_a$) or the coordinating ability of the conjugate base.[18] It is therefore very likely that **1** has a p$K_a$ value higher than the mineral acids such as HCl. In comparison with the strong organic acids such as trifluoroacetic acid and pentadifluoropropionic acid, **1** has similar acid strength as the fluoroalkyl acids that react reversibly with Vaska's complex to give multiple isomers[19] as observed with **1**. The labile nature of the $N_2$ ligand in *trans*-Ir(Cl)($N_2$)($PPh_3$)$_2$ also facilitates the eventual bidentate coordination of the nitrogen acids, which is not possible for the more inert carbonyl complex. During the course of the reaction, transient intermediates are observed in the $^{31}$P and $^{1}$H NMR spectra, which will be discussed later.

**Structural Results.** The solid-state molecular structures for the nitrogen acids **1**, **3**, and **4** are shown in Figure 2.

Compound **1** is shown to adopt the Z conformation in the solid state similar to **2**. However, DFT calculations indicate that the most stable gas-phase isomer is the E isomer (Figure 3a). For **3**, the Z isomer is calculated to be only slightly more stable, which is the same as that observed in the solid state (Figure 3b).

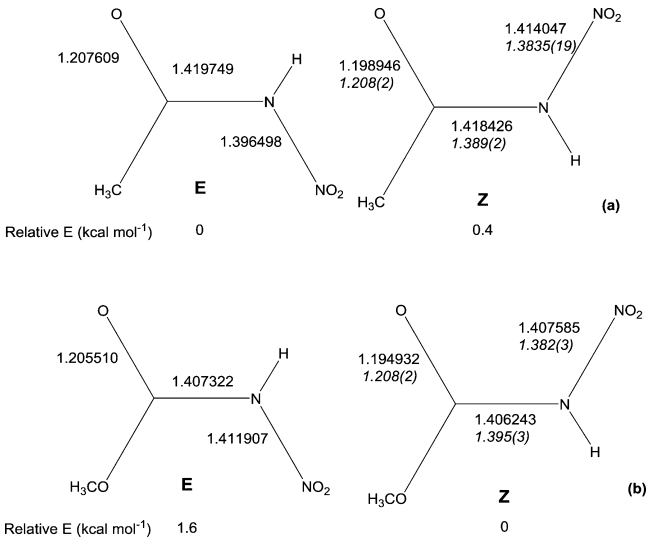


**Figure 3.** DFT calculated bond lengths and relative energy levels of the isomers of (a) **1** and (b) **3**. Measured bond distances are shown in italics.

A list of selected experimentally determined bond lengths and bond angles of the free ligands of the nitrogen acids are presented in Table 1. In general, all the molecules are planar with most of the dihedral angles around the amide/carbamate groups at or close to 180°. The planarity and the short C–N, 1.38 to 1.40 Å, and N–N, 1.38 to 1.40 Å, bond lengths of these acids is consistent with considerable delocalization of the N lone pair across the framework. An interesting observation in this series of compounds is that the N-nitrocarbamates **3** and **4** are slightly nonplanar due to deviations from 0 or 180° in the dihedral angles of C–C–N–O and C–N–N–O. This could be the result of competing conjugation requirements of the carbamate functional group. Increasing the alkyl chain length of the alkoxy group seems to reduce the planarity too.

Although the bond angles of the N-nitro compounds are similar, for the nitro groups the N–N–O angles for the nitro group are different. The O(1) atom, which is trans to the acyl group, tends to have smaller N–N–O angles compared to the O(2) atom cis to the acyl group. This asymmetric effect could be due to packing constraints. The presence of extensive hydrogen bonds between the amide protons and the acyl oxygen atoms in the crystal array, which stabilize the Z conformation in **1**, may also lead to these variations in nitro group geometry.

The molecular structures of **5**, **6**, and **7** are shown in Figure 4. In all of the three examples, the new Ir(III) complexes have a distorted octahedral geometry with the triphenylphosphine ligands trans to each other. The Ir(III) complexes are shown to have an unexpected bidentate coordination of the N-nitro-amide/carbamate conjugate base through the nitrogen on the amide functionality and the oxygen of the nitro group. The nitrogen acid conjugate bases form a four-membered Ir–N–N–O chelate ring. The chloride ligand is positioned trans to the N atom of the amide group with Cl(1)–Ir(1)–N(1) between 164° to 173°. The most interesting aspect of the solid-state structures for the complexes is that one of the oxygen atoms of the nitro group out-competes the acyl oxygen that is present in **5** and **6** as well as an additional methoxy subsituent in **7** for coordination to the Ir center (Figure 4). Our previous report for **6** had included a comparison of the different isomers with DFT calculations.[3] For **7**, the oxygen of the alkoxy group can also coordinate to the Ir center giving four additional possible isomers; however, the preferred mode of coordination is still the oxygen of the nitro group.

A different type of isomerism encountered within these Ir(III) complexes involves the nitrogen acid ligands. As discussed above, there are two possible conformations for the nitrogen acids, E or Z. On the basis of conventions, the E/Z isomerism for ligands coordinated to transition metal complexes may be different from the free acid or the anionic salts (Figure 5).

For **5** and **6**, the N-nitroamide conjugate base has a flipped geometry around the C–N bond, while for **7** the ligand C–N conformation corresponds to that also found in the free acid **3**.

The selected structural data for **5**, **6**, and **7** are shown in Table 1. The Ir(1)–N(1) bond length for all three complexes are approximately 2.04 Å, which corresponds to an Ir–N single bond. The Ir(1)–O(1) bond lengths of the three complexes are more than 2.33 Å, which is longer than most Ir–O single bonds and indicates a weak Ir–O bond. The reason for the observed structural feature may be due to the trans influence of the hydride ligand.[20] The N(1)–N(2) bond lengths of **5** and **7** decreased on coordination to the Ir center in comparison to the


dx.doi.org/10.1021/ic5017033 | Inorg. Chem. 2014, 53, 11160–11172

**Table 1. Selected Bond Lengths (Å) Bond and Torsion Angles (deg) of N-Nitroamides, N-Nitrocarbamates, and Ir($\eta^2$-X)(H)(Cl)($PPh_3$)$_2$ Complexes from X-ray Diffraction**

| compound | 1 | 2[3] | 3[a] | 4 | 5 | 6[b] | 7 |
|---|---|---|---|---|---|---|---|
| N(1)−N(2) | 1.3835(19) | 1.3858(18) | 1.382(3)/1.380(3) | 1.385(2) | 1.372(5) | 1.389(6) | 1.349(4) |
| N(1)−C(1) | 1.389(2) | 1.3949(19) | 1.394(3)/1.396(3) | 1.387(2) | 1.398(6) | 1.372(7) | 1.405(5) |
| N(2)−O(1) | 1.2230(17) | 1.2183(16) | 1.222(3)/1.226(3) | 1.216(2) | 1.287(5) | 1.298(6) | 1.275(4) |
| N(2)−O(2) | 1.2144(17) | 1.2141(16) | 1.212(3)/1.214(3) | 1.2154(19) | 1.199(5) | 1.193(6) | 1.223(4) |
| Ir(1)−N(1) | | | | | 2.030(3) | 2.042(4) | 2.050(3) |
| Ir(1)−O(1) | | | | | 2.329(3) | 2.357(4) | 2.323(3) |
| N(1)−N(2)−O(1) | 114.14(12) | 114.40(11) | 114.0(2)/113.9(2) | 115.17(14) | 109.4(3) | 109.6(4) | 110.8(3) |
| N(1)−N(2)−O(2) | 119.62(13) | 119.18(11) | 119.7(2)/119.3(2) | 118.41(15) | 128.1(4) | 126.6(5) | 126.5(3) |
| N(2)−N(1)−C(1) | 125.47(13) | 125.27(12) | 124.5(2)/124.6(2) | 123.87(14) | 121.9(4) | 120.7(5) | 118.9(3) |
| O(1)−N(2)−O(2) | 126.24(13) | 126.42(12) | 126.3(2)/126.8(2) | 126.41(16) | 122.5(4) | 123.8(5) | 122.7(4) |
| Ir(1)−N(1)−N(2) | | | | | 101.2(2) | 101.3(3) | 100.4(2) |
| O(1)−Ir(1)−N(1) | | | | | 59.26(12) | 59.38(16) | 58.80(11) |
| N(2)−O(1)−Ir(1) | | | | | 90.1(2) | 89.7(3) | 89.97(19) |
| O(1)−N(2)−N(1)−C(1) | 180.0(1) | 180.0(1) | −178.2(2)/-178.8(2) | 168.1(2) | 173.7(4) | −179.9(5) | 178.3(4) |
| O(3)−C(1)−N(1)−N(2) | 0.0(2) | 0.0(2) | −1.3(4)/0.5(4) | −1.8(3) | −174.3(4) | 173.3(5) | −1.2(7) |

[a] **2** independent molecules. O(5), O(6), O(7), O(8), N(3), N(4), C(3), C(4) in corresponding order for second molecule. [b] Atom sequence of complex **6** has been change from reference 3

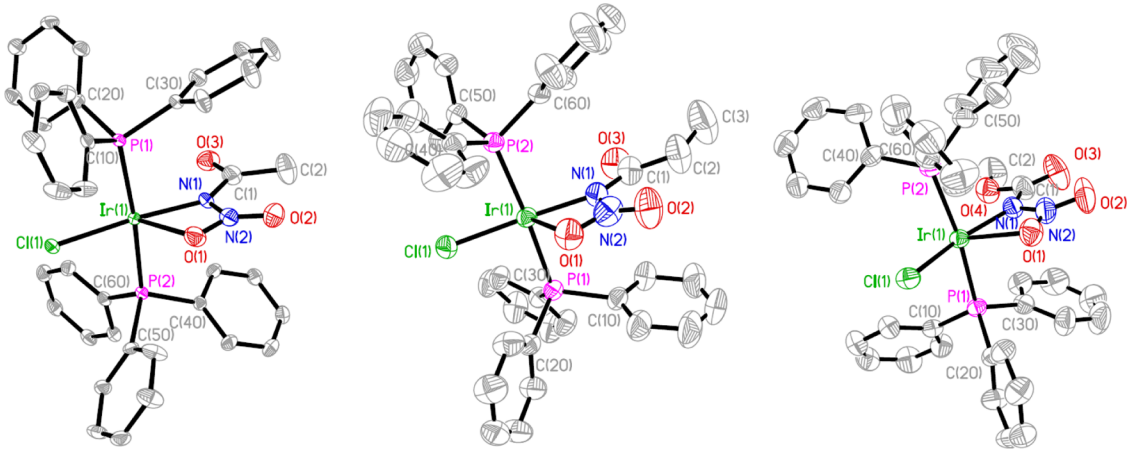


**Figure 4.** Molecular structures of (a) **5** at 45% thermal ellipsoid, (b) **6** and (c) **7** at 50% thermal ellipsoid. Hydrogen atoms and solvent molecules were omitted for clarity.

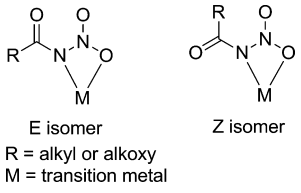


**Figure 5.** E/Z isomers of nitrogen conjugate acids coordinated to transition metal.

free acid **1** and **3**. For **6**, the N(1)−N(2) bond length is similar to that of **2**. The N(1)−C(1) bond lengths of **5** and **7** both increased compared to **1** and **3**. For **6**, a reverse in the trend is observed as the N(1)−C(1) bond length actually decreases compared to **2**.

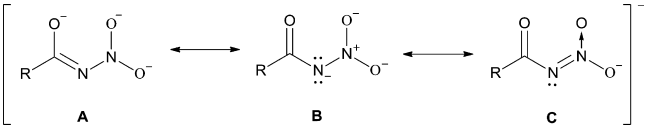


The N−O bond lengths in **5**, **6**, and **7** differ significantly between the metal-bound N(2)−O(1) and the free N(2)−O(2) by at least 0.5 Å. This represents a more localized bonding arrangement for the shorter noncoordinating N−O fragment, resonance form **C**, which is formally the N-oxide of the acetyldiazotate anion. The bite angle of the Ir−N(1)−N(2)−O(1) chelate is typical of four-membered rings, which is very acute compared to five- or six-membered rings. This bonding mode is, however, preferred in these systems even though alternative less-strained chelate rings are possible with the acyl group. The length of the alkyl chain on the acyl fragment does not have a significant effect on the planarity between the amide and nitro section of the nitrogen acid ligands on coordination.

**Dynamic Process in Solution.** As mentioned above, the observation of the $^1$H NMR Ir−H resonance signal confirms the presence of a metal hydride, which is not located in the X-ray diffraction experiments. However, the appearance of a broad signal for the Ir−H resonance in **5** is unexpected. A broad NMR signal could be due to the presence of a


dx.doi.org/10.1021/ic5017033 | Inorg. Chem. 2014, 53, 11160−11172

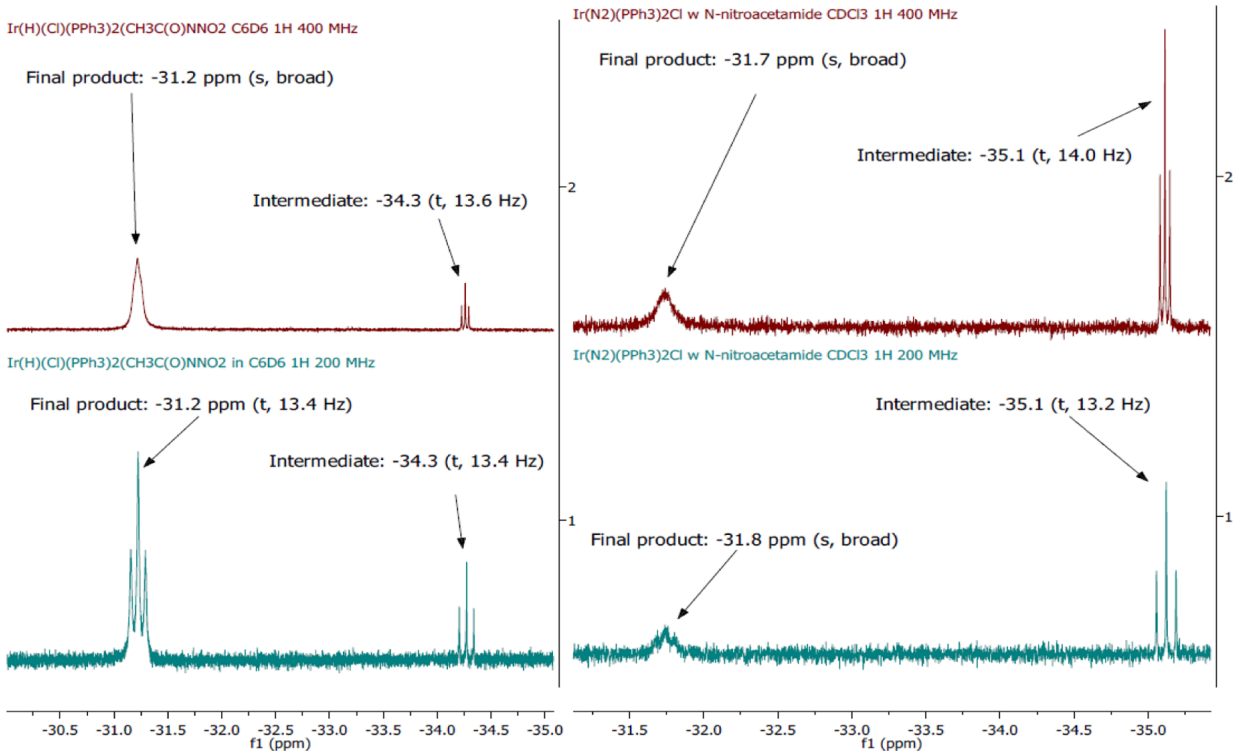


**Figure 6.** Variable-field $^{1}$H NMR 400 MHz (upper) and 200 MHz (lower) in $C_6D_6$ (left) and $CDCl_3$ (right) for Ir−H region of **5** shown with presence of the transient species.

paramagnetic metal center or a dynamic process occurring in solution. The Ir(III) metal centers have a low-spin $d^6$ configuration, and coupled with the general sharp signals observed in the rest of the NMR spectra, the latter is more likely. For **5**, the appearance of the broad signal is also solvent-dependent (Figure 6).

The additional metal hydride resonance that is located further upfield at approximately −35 ppm in Figure 6 is a separate species that does not interact with the product resonance at −30 ppm as both of the resonance signals broaden and resolve independently. This upfield resonance is assigned to an intermediate (see below).

In $CDCl_3$, at the effective field strength of 200 MHz, the Ir hydride signal is very broad, but this sharpens slightly when the effective field strength is increased to 400 MHz. When $C_6D_6$ is used instead, the Ir hydride signal is observed to be a triplet at the effective field strength of 200 MHz. When the effective field strength is increased to 400 MHz, the same signal is now observed as a broad signal. The conclusion for the observations is that in $C_6D_6$ the dynamic process is at the fast-exchange limit. In $CDCl_3$, the dynamic process is also at the fast-exchange limit but is closer to the lower coalescence temperature; at effective field strength of 200 MHz, the lower coalescence temperature has already been breached giving a broad signal that sharpens as the effective field strength is increased. It is likely that the dynamic process is faster in $C_6D_6$ than it is in $CDCl_3$.

From the collective Ir hydride resonances observed for **5**, **6**, **7**, and **8**, it is very likely that an increase in the alkyl chain length or change to an alkoxy chain length causes the rate of the dynamic process to increase such that all the triplet resonances observed are actually in the fast-exchange region. This is supported to some extent since the Ir hydride resonance signal in **6** is a broad signal that shows some coupling pattern that can be resolved as a triplet (Supporting Information, Figure S3).[3]

Since the broad resonance is only observed for the Ir hydride and neither in the other proton resonances nor in the $^{31}$P NMR, it is very likely that the dynamic process significantly affects the Ir−H environment. We propose that this dynamic process is due to a labile reversible O atom coordination trans to the hydride (Scheme 4). The reason for such a phenomenon could be due to the strong trans effect of the hydride ligand.[20]

**Scheme 4. Proposed Labile Coordination of O Atom to Ir Center**

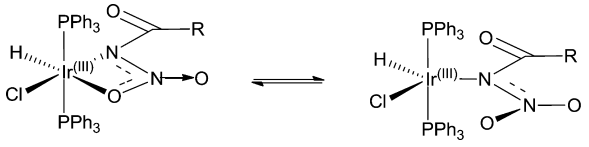

The related Ir(III) acetate complex, $Ir^{III}(\eta^2\text{-}CH_3CO_2)(H)(Cl)(PPh_3)_2$ (**12**), synthesized by Kubota and co-workers, was prepared and does not exhibit this fluxional behavior in either the $^{31}$P or $^{1}$H spectra (Supporting Information).[21] The Ir hydride signal observed in **12** stands in stark contrast with that of **5** and provides more evidence for the dynamic behavior of **5** in solution.

**Reaction Intermediates and Transient Species.** In the course of treating *trans*-$Ir(Cl)(N_2)(PPh_3)_2$ with **1** to give **5**, a transient species is observed to form initially, which slowly converts into the final product, which is isolated in excellent yield. This intermediate, **5A**, can be observed using $^{31}$P NMR (Figure 7), $^{1}$H NMR (Figure 8), and solution IR (Figure 9) spectroscopy techniques. In this and subsequent discussion the term intermediate is used for the transient species that are observed to form and then convert to the final product and are not isolated.


dx.doi.org/10.1021/ic5017033 | *Inorg. Chem.* 2014, 53, 11160−11172

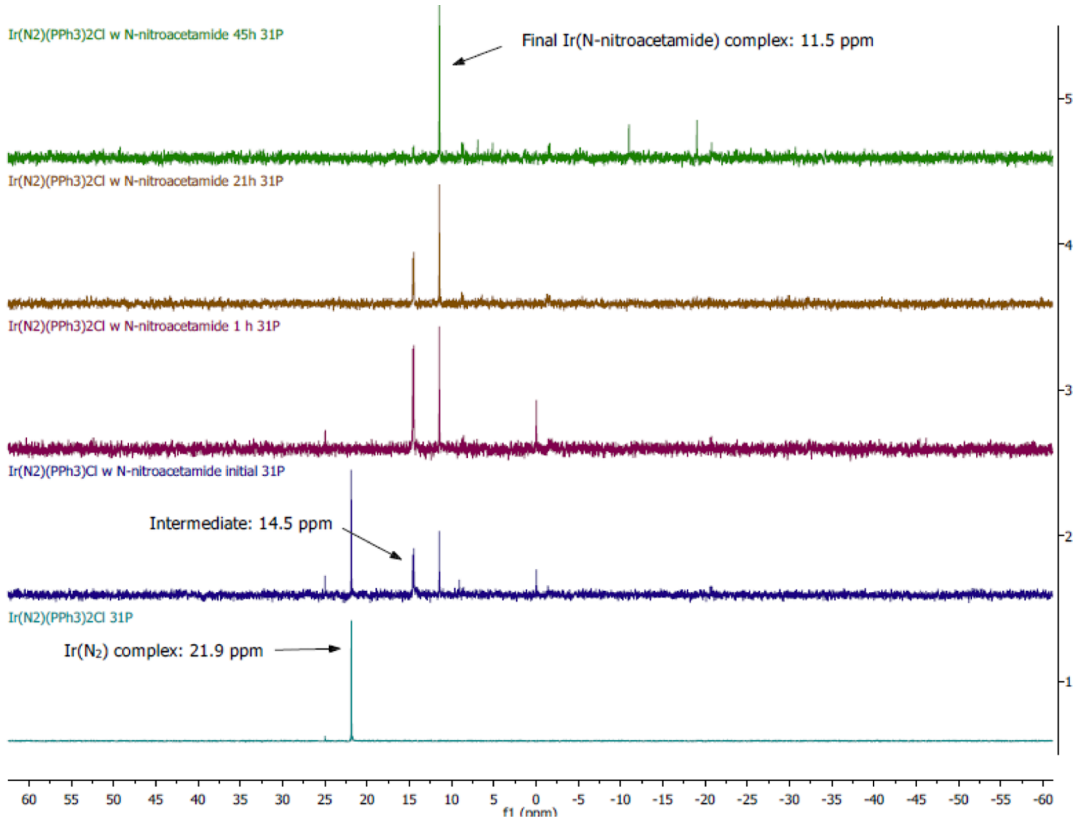


**Figure 7.** $^{31}$P NMR reaction monitoring of *trans*-Ir(Cl)$(N_2)(PPh_3)_2$ with **1** in $CDCl_3$ to give **5**.

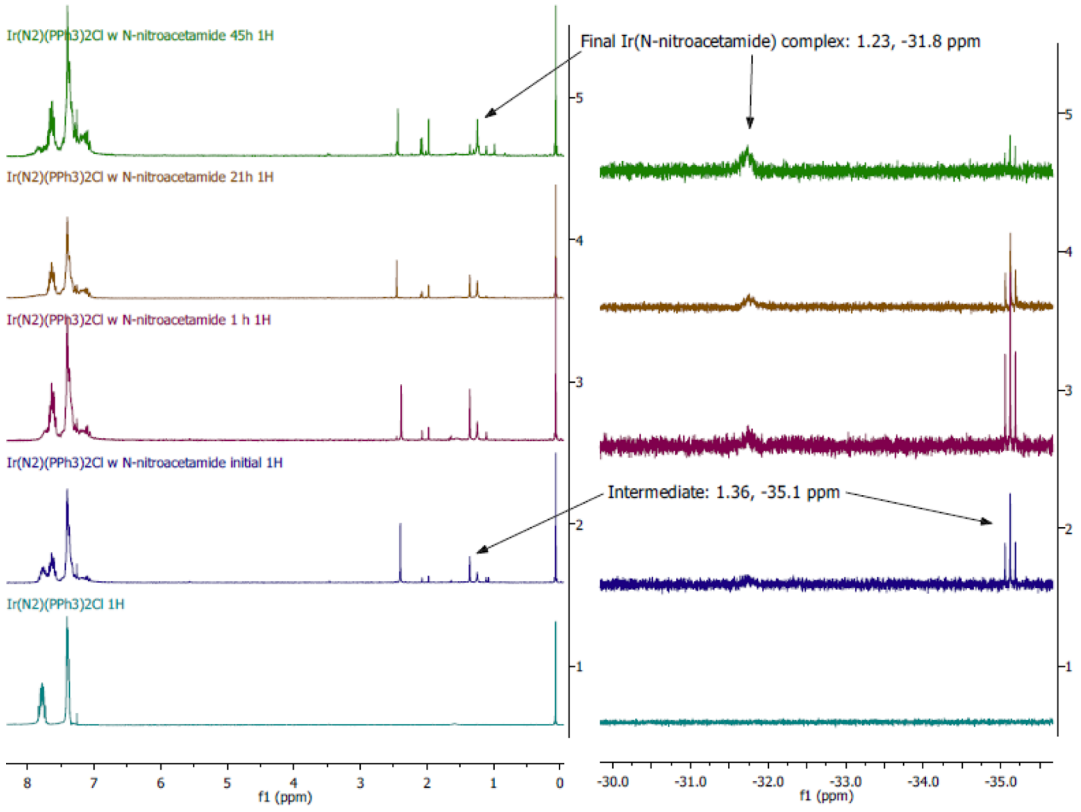


**Figure 8.** $^{1}$H NMR reaction monitoring of *trans*-Ir(Cl)$(N_2)(PPh_3)_2$ with **1** in $CDCl_3$ to give **5**.

In $^{31}$P NMR (Figure 7), a resonance signal at 14.5 ppm is observed to form initially together with the signal at 11.5 ppm. The 14.5 ppm signal initially increases and subsequently decreases over time to give only the signal at 11.5 ppm. Thus,


dx.doi.org/10.1021/ic5017033 | *Inorg. Chem.* 2014, 53, 11160−11172

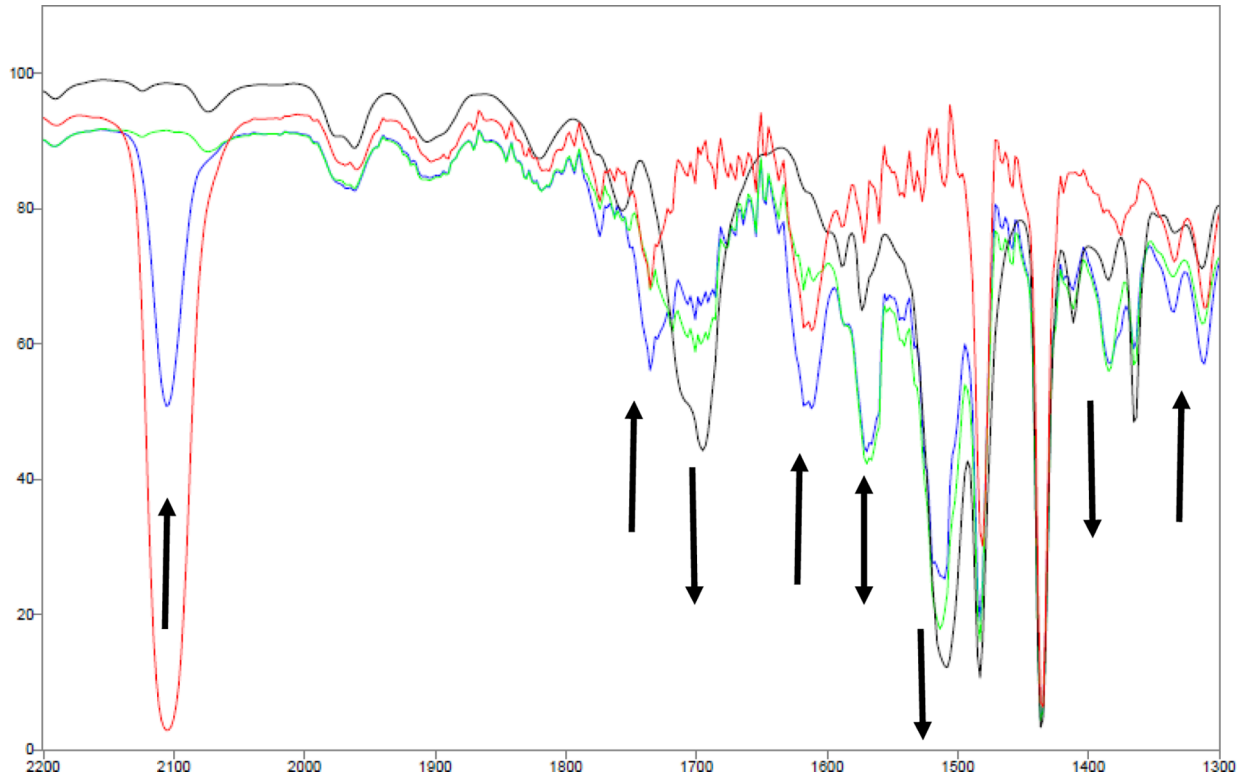


**Figure 9.** Solution IR spectra for the reaction of *trans*-Ir(Cl)($N_2$)($PPh_3$)$_2$ with **1** to give **5** between 2200 and 1300 $cm^{-1}$. Reaction carried out at −10 °C in $CHCl_3$ over 24 h. Aliquots taken at the following time intervals: (red) Initial *trans*-Ir(Cl)($N_2$)($PPh_3$)$_2$ complex immediately after addition of **1**; (blue) after 15 min; (green) after 1.5 h; (black) after 17 h.

the signal at 14.5 ppm corresponds to an intermediate that slowly converts to **5**, which is at 11.5 ppm. This similar trend is also observed in $^1$H NMR (Figure 8), where the resonance signals at 1.36 and −35.1 ppm assigned to **5A** increased and subsequently decrease to resonance signals at 1.23 and −31.8 ppm observed in **5**.

The multiple solution IR spectra of the reaction mixture over time gave the most information regarding the functional group changes taking place over time (Figure 9). It is shown that the band at 2104 $cm^{-1}$ corresponding to the $N_2$ band in *trans*-Ir(Cl)($N_2$)($PPh_3$)$_2$ rapidly disappears, which indicates the loss of $N_2$ ligand. Similar bands at 1736 and 1610 $cm^{-1}$, which belong to **1** and a band near 1300 $cm^{-1}$, are also observed to decrease overtime. The band at 1570 $cm^{-1}$ is observed to increase initially but decrease over the course of the reaction. Finally product bands at 1695, 1510, and 1360 $cm^{-1}$ are observed to increase over time.

We conclude that the band at 1570 $cm^{-1}$ most likely corresponds to **5A** that is observed in the $^{31}$P and $^1$H NMR spectra. Comparing the IR bands in some carboxamide complexes[22] and the related Ir(III) carboxylate complexes such as **12**,[21] the 1570 $cm^{-1}$ band may be assigned to a coordinated acyl ligand. Togther with the NMR data obtained, a few possible conformations of the intermediate are proposed (Figure 10).

The reaction of *trans*-Ir(Cl)($N_2$)($PPh_3$)$_2$ with **3** to give **7** was also monitored by $^{31}$P NMR (Supporting Information, Figure S4), $^1$H NMR (Supporting Information, Figure S5), and IR spectroscopy (Supporting Information, Figure S6) and reveals the possible presence of two species that eventually convert to the product **7**.

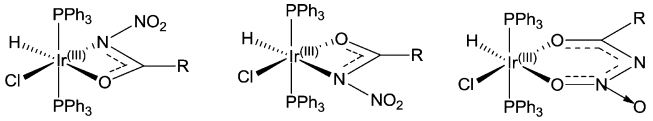


**Figure 10.** Possible structures for the intermediates observed in *trans*-Ir(Cl)($N_2$)($PPh_3$)$_2$ reaction with **1** and **3** to give **5** and **7**, respectively.

The $^{31}$P NMR is observed to show two transient species, namely, **7A** at 14.4 ppm and **7B** at 7.5 ppm, with intermediate **7B** in greater proportion. Both these intermediates are observed to disappear within 3 h to give **7**, which has the resonance signal at 10.0 ppm. Similarly, in $^1$H NMR, resonances corresponding to the transient species are observed; **7A** at 3.4 and −36.7 ppm and **7B** at 3.6 and −26.0 ppm with **7B** in greater proportion. These resonances disappear over time to give resonance signals at 3.0 and 35.7, which are assigned to **7**.

The solution IR monitoring formation of **7** reveals some similar changes observed in the synthesis of **5**. The decrease of the 2104 $cm^{-1}$ band of the starting $N_2$ ligand with concurrent decrease in the 1790 and 1620 $cm^{-1}$ bands are assigned to **3**. The increase in the bands at 1750 and 1260 $cm^{-1}$ and the general increase in the bands between 1570 and 1500 $cm^{-1}$ are due to the formation of **7**. In this case, no initial increase and subsequent decrease and loss of any bands could be observed. A possible reason is that the rate of reaction of *trans*-Ir(Cl)($N_2$)($PPh_3$)$_2$ with **3** is much more rapid than it is with **1**. This is shown by the rapid loss of the 2104 $cm^{-1}$ band and the overall time scale of the transformations. In the reaction of


dx.doi.org/10.1021/ic5017033 | *Inorg. Chem.* 2014, 53, 11160−11172

**Scheme 5. Reaction of Methyl Triflate with 5 To Form 9**

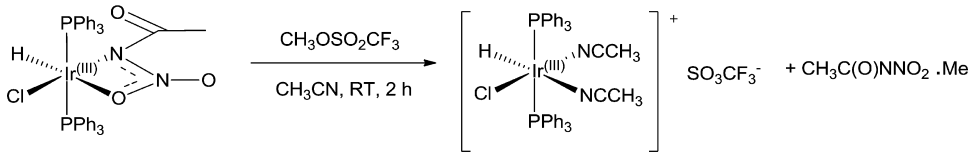


5 9

*trans*-Ir(Cl)$(N_2)(PPh_3)_2$ with **1**, the reaction time monitored in NMR is over 24 h long, while that with **3** is observed to be complete within 2 h! Thus, despite starting the solution IR experiment at −10 °C, the rate of conversion between the intermediates to **7** was too rapid for observation of significant quantities of any transient species.

The possible structures of the intermediates **7A** and **7B** are shown in Figure 10, which corresponds with the spectroscopic data. With the limited data, it is not possible to determine if intermediates **7A** and **7B** interconvert between them to give **7**.

The key difference between the formation of **5** versus that of **7** is that the rate of conversion of the intermediates in **7** is much faster than that of **5**. This difference may be driven by the alkoxy versus the alkyl functional group or may reflect the different p$K_a$ of the free acids.

We were unsuccessful in obtaining the crystal structure for **8**; however, from the $^{31}P$ and $^{1}H$ NMR reaction monitoring results (Supporting Information, Figures S7 and S8, respectively) together with the IR results of the isolated solids, it is determined that **8** has similar reaction intermediates and product geometry as **7**. Thus, the structure of **8** is very likely an analogue of **7** with an ethoxy group.

**Reactivity Studies of Ir($\eta^2$-$CH_3C(O)NNO_2$)(H)(Cl)$(PPh_3)_2$ (5).** Upon methylation with methyl triflate **5** there is a loss of the N-nitroacetamide ligand, to give the bis(acetonitrile) Ir(III) complex **9** (Scheme 5).

The IR spectrum of **9** shows multiple weak bands in the 2270 $cm^{-1}$ region, which can be assigned to the coordinated acetonitrile ligands and the Ir hydride stretch. The appearance of the bands at 1270, 1154, 1031, and 638 $cm^{-1}$ confirms the presence of the triflate anion, while the disppearance of bands at 1695, 1514, 1262, 1198, and 621 $cm^{-1}$ indicates the loss of the coordinated N-nitroacetamide ligand. The $^{31}P$ spectrum shows only a single singlet at 4.43 ppm, and the $^{1}H$ NMR spectrum has only a single triplet at −20.67 ppm for the Ir hydride, indicating a single species. New singlets at 1.90 and 2.00 ppm can be assigned to the methyl in the coordinated $CH_3CN$ ligands. A crystal structure determination for **9** confirms the above assignments (Supporting Information, Table S1 and Figure S2).

The methylation of **5** only occurs in acetonitrile and is unsuccessful in other solvents such as $CHCl_3$ and benzene. The use of alternative methylating agents such as $CH_3I$ and dimethylsulfate did not alter the reaction outcome in other solvents. It is very likely that coordination of the acetonitrile ligand to **5** is necessary for the methylation reaction to proceed and is related to the proposed labile behavior of the coordinated oxygen atom of the nitro group. It is interesting that successful methylation of the N-nitroacetamide ligand results in the loss of the methlylated ligand through substitution by acetonitrile. We were not able to isolate the methylated N-nitroacetamide ligand but propose the methylation site to be on the oxygen atom of the nitro group. Attempts to identify the methylation product of the conjugate base of **1** were unsuccessful using chemical ionization/ESI-MS or GC-MS of the reaction mixture.

Tertiary phosphines react rapidly but incompletely with **5**. For example, 1 equiv of $P(CH_3)_2Ph$ did not result in conversion of all starting complex. Complex **5** was still dominant after extended reaction times. Several new $^{31}P$ NMR resonance signals were observed, one of which with significant intensity at −4.38 ppm is assigned to free $PPh_3$. A set of doublet and triplet signals with similar coupling constants of 19.9 Hz in the $^{31}P$ NMR spectrum represents a phosphine ligand that is positioned cis to two identical trans phosphine ligands. It is very likely that the initial substitution to one of the $PPh_3$ ligands of **5** results in the phosphine-substituted product to be more reactive toward further $PPh_3$ substitution. (Scheme 6)

**Scheme 6. Proposed Reaction Isomers of 10 from the Addition of $P(CH_3)_2Ph$ to 5 with Fractional Proportions**

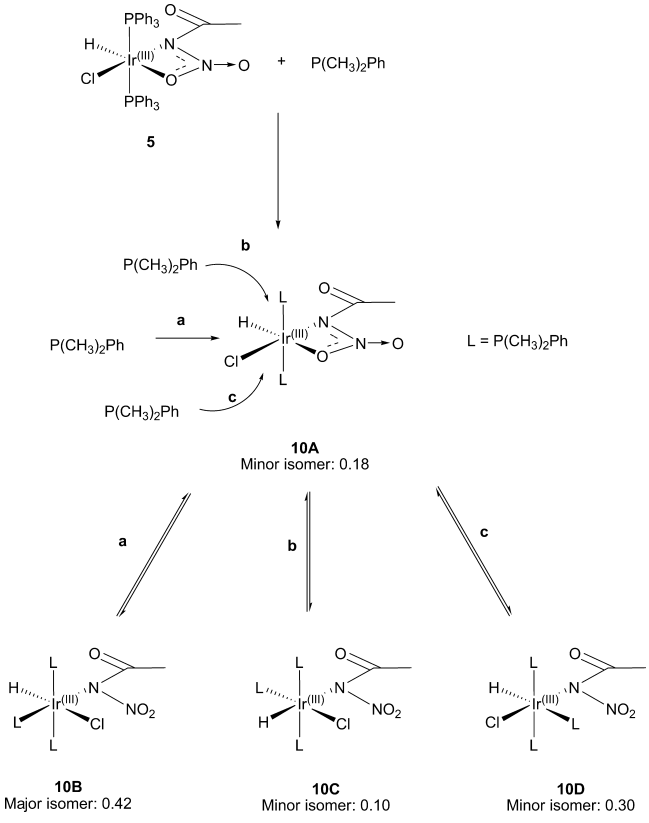


This is supported by the absence of two sets of doublets that have large coupling being observed in the $^{31}P$ NMR for inequivalent trans phosphines. The substituted phosphine complex **10A** also undergoes further nucleophilic addition of an additional $P(CH_3)_2Ph$ molecule preferentially to give the isomers **10B**, **10C**, and **10D**. This is evidenced by the


dx.doi.org/10.1021/ic5017033 | *Inorg. Chem.* 2014, 53, 11160−11172

appearance of three sets of doublets of triplets resonance signals and a single triplet in the upfield region of the $^1$H NMR spectrum. With excess $P(CH_3)_2Ph$ added, total conversion of **5** occurs to give the four complexes. The single Ir hydride triplet is assigned to the $PPh_3$ substituted **10A** as it is not coupled to any additional phosphine.

The three complexes, **10B−D**, will have identical $^{31}$P NMR coupling systems and are assigned to the doublet and triplet resonance signals (Scheme 6). One of the doublet of triplet $^1$H signals for the Ir hydride complexes has a significantly large doublet coupling constant of 158 Hz. This isomer is most likely **10D**, which has the hydride located trans to the dimethylphenylphosphine ligand. The remaining two hydric doublet of triplets have the hydride located cis to the equatorial phosphine, and the assignment of the signals assumes that $P(CH_3)_2Ph$ preferentially adds from the less-hindered site. Therefore, **10B** is formed in larger proportions than **10C**.

For the corresponding carboxylate complex **12**, addition of $P(CH_3)_2Ph$ gives only a single isomer of $Ir(\eta^1\text{-}CH_3CO_2)(H)(Cl)(P(CH_3)_2Ph)(PPh_3)_2$ (**13**), with the Ir hydride trans to the $P(CH_3)_2Ph$ ligand.[21] The original article characterized this isomer by its $\nu$(Ir−Cl). A separate synthesis[21] of **13** confirms the presence of $\nu$(Ir−H) at 2187 cm$^{-1}$. The $^{31}$P NMR contains two sets of resonances, namely, a doublet at −2.77 ppm (13.5 Hz) assigned to $P(CH_3)_2Ph$ and a triplet of doublet at −42.50 ppm assigned to $PPh_3$ from coupling to both the P (13.5 Hz) and $CH_3$ groups (7.3 Hz) in $P(CH_3)_2Ph$. Significantly, these NMR results confirm only one isomer is present.

The carbonylation of **5** gives a single new broad IR band at 2047 cm$^{-1}$ This band is assigned to the carbonyl ligand of the new Ir(III) carbonyl complex **11**. The Ir hydride stretch is also observed as a low-intensity broad band centered at 2185 cm$^{-1}$. The $^{31}$P and $^1$H NMR spectra, however, indicate the presence of multiple isomers of **11**. In the $^{31}$P NMR spectrum, two resonance signals are observed with unequal intensity. In the $^1$H NMR, three Ir hydride triplet resonances are observed, with two signals that are significantly stronger and the third weaker in a ratio of 0.56:0.39:0.05. Thus, there are three isomers of **11** that can form depending, on the site of CO addition (Scheme 7).

**Scheme 7. Possible CO Addition Coordination Isomers with 5**

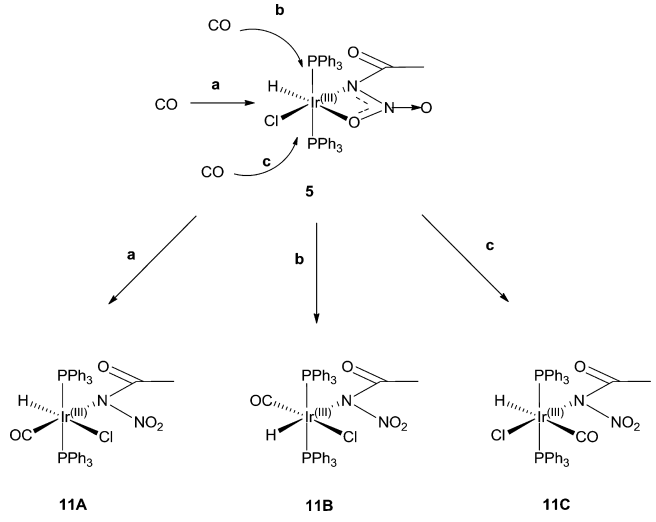


The carboxylate complex **12** also undergos CO addition to give $Ir(\eta^1\text{-}CH_3CO_2)(H)(Cl)(CO)(PPh_3)_2$ (**14**).[21] Complex **14** is reported to be only one isomer based on IR analysis of the Ir−H, Ir−Cl, and Ir-CO stretches. The trans labilization effect of carbon monoxide[23] on the Ir hydride affects $\nu$(Ir−H) stretch that is found at 2112 cm$^{-1}$, which is much lower than that of **12** at 2307 cm$^{-1}$. The observation of hydridocarbonyl vibrational coupling[24] also supports a trans H−Ir−CO structure from isotopic analysis using $^1$H/$^2$D Ir hydride samples. The $^{31}$P single singlet resonance at 5.41 ppm, $^1$H NMR signals of singlet at 1.06 ppm for the methyl group, and triplet at −7.83 ppm (14 Hz) for the Ir hydride indicate the presence of only a single isomer for **14**.

The formation of multiple isomers in **11** compared to **14** could be due to the labile coordination of the oxygen of the nitro group. Isomeric carbonyl complexes of **11** are metastable and reversibly lose CO to regenerate **5**. Ir(III) complexes with a labile carbonyl are rare, but there are precedents of labile CO on transition metal complexes such as the d$^6$ $Re(\eta^1\text{-}CH_3CO_2)(CO)_3(PPh_3)_2$ complex.[25] The presence of three $\pi$-accepting CO ligands causes the Re center to be electron-deficient resulting in a labile CO. Thus, the electron-withdrawing or $\pi$-backbonding effect of the N-nitroacetamide ligand may be the cause for the hemilabile nature of CO and substitution of $PPh_3$ by $P(CH_3)_2Ph$. Furthermore, the bidentate nature of the N-nitroacetamide ligand allows efficient chelation to the Ir center. These two factors together may play a role in the labile nature of the carbonyl ligand.

The reactivity studies of **12** are in great contrast with **5** with regard to CO and $P(CH_3)_2Ph$ addition. In both the CO and $P(CH_3)_2Ph$ additions to **12** only one ligand is added to generate single isomers, which are stable. For **5**, the addition of $P(CH_3)_2Ph$ results in $PPh_3$ substitution by $P(CH_3)_2Ph$, which is further observed to preferentially add an additional $P(CH_3)_2Ph$ to give isomers of **10**. The introduction of CO to **5** generates isomers of **11**, which on prolonged duration in solution loses CO and regenerates **5**. The above reactivity for **5** can be attributed to both the electron-withdrawing nature of the N-nitroacetamide ligand and the labile coordination of the oxygen atom of the nitro group observed earlier from the $^1$H NMR of the Ir hydride resonance. It seems that the trans labilizing effect of the Ir hydride[20] in **5** is not sufficient to enforce the formation of a single isomer for nucleophiles.

The carbon monoxide addition reaction to **5** to give isomers of **11** is in contrast to the reaction of *trans*-$Ir(Cl)(CO)(PPh_3)_2$ with **1** (Scheme 8). The former results in formation of isomers that reversibly lose the CO ligand, while the latter gives incomplete conversion of the starting complex *trans*-$Ir(Cl)(CO)(PPh_3)_2$, which, with excess amounts of **1**, generates multiple products. Significantly, reductive elimination of the conjugate base of the nitrogen acid ligand to give Vaska's complex is not observed.

## CONCLUSION

Compounds **1−4** undergo oxidative addition with *trans*-$Ir(Cl)(N_2)(PPh_3)_2$ to give new Ir(III) hydrido nitrogen acid complexes **5−8**, respectively, which exhibit diagnostic vibrational bands. The Ir(III) complexes all feature an unusual four-membered N,O chelate with the nitrogen of the amide and the oxygen of the nitro group to the Ir center. The $^1$H NMR spectrum for **5** is observed to have solvent-dependent line shape behavior for the metal hydride resonance, which can also be observed on varying the effective field strength. This effect is


dx.doi.org/10.1021/ic5017033 | Inorg. Chem. 2014, 53, 11160−11172

**Scheme 8. Reaction of 5 with CO Versus Reaction of *trans*-Ir(Cl)(CO)$(PPh_3)_2$ with 1**

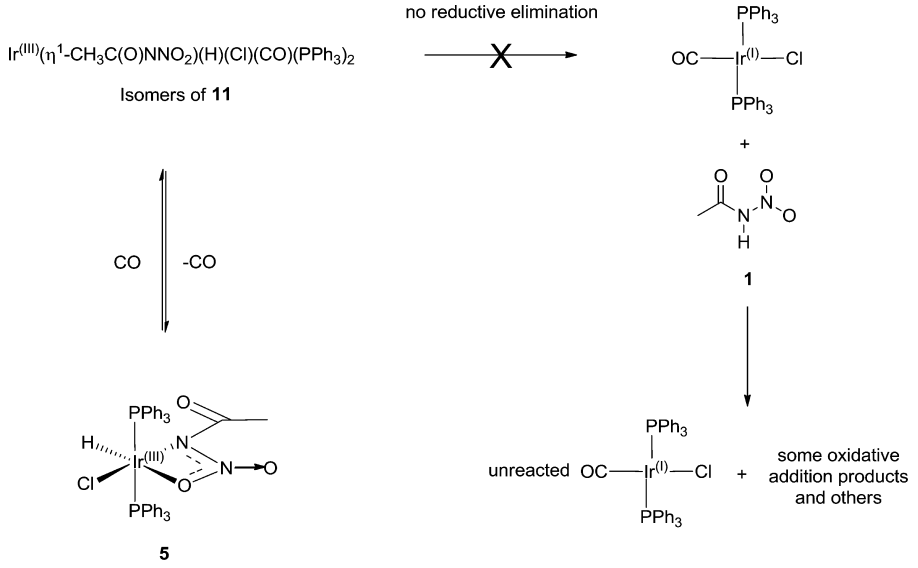


proposed to be due to the labile Ir−O bond and is believed to undergo rapid coordination and release in solution. The fluxional behavior of the nitrogen acid in **5** is believed to contribute to the unusual reactivity with nucleophiles such as $P(CH_3)_2Ph$ and carbon monoxide to give multiple isomers. Particularly significant is the ability of the Ir(III) carbonyl isomeric complexes of **11** to lose the carbonyl ligand over time in solution. The methylation reaction of **5** is only possible in acetonitrile and results in the loss of the conjugate acid of **1** with the formation of the bis(acetonitrile) complex **9**. The reaction profiles for the nitrogen acids with *trans*-Ir(Cl)$(N_2)$-$(PPh_3)_2$ were also monitored using solution IR and $^1H$ and $^{31}P$ NMR spectroscopies and are observed to give rise to at least one intermediate.

## ■ ASSOCIATED CONTENT

### Supporting Information

Information on the crystallographic parameters of the determined structures, ORTEP plot of **9**, NMR and IR reaction profile of **7** and **8** are included. NMR characterization of the transient species in the syntheses of **5**−**8** are also included. This material is available free of charge via the Internet at http://pubs.acs.org. The CIF files for the X-ray structure determinations of **1**, **3**, **4**, **5**, **7**, and **9** are available at CCDC with the following code numbers 948801, 948805, 948803, 948802, 948804, and 1012233 respectively.

## ■ AUTHOR INFORMATION

### Corresponding Author

*Email: Scott.Bohle@mcgill.ca.

### Notes

The authors declare no competing financial interest.

## ■ ACKNOWLEDGMENTS

We would like to thank C. Campana for helpful discussion regarding the X-ray diffraction solution of **5**. We gratefully acknowledge the CRC, CFI, and NSERC for support in the forms of CRC, CFI, and discovery grants to D.S.B.

## ■ REFERENCES

(1) (a) Dyker, G. In *Coupling reactions involving CH activation;* Wiley-VCH Verlag GmbH: Hoboken, NJ, 1998; pp 241−250;. (b) Crabtree, R. H. *Pure Appl. Chem.* **2003**, *75*, 435−443. (c) Crabtree, R. H. *J. Organomet. Chem.* **2004**, *689*, 4083−4091. (d) Hashiguchi, B. G.; Bischof, S. M.; Konnick, M. M.; Periana, R. A. *Acc. Chem. Res.* **2012**, *45*, 885−898. (e) Girard, S. A.; Knauber, T.; Li, C.-J. *Angew. Chem., Int. Ed.* **2014**, *53*, 74−100.

(2) (a) Casalnuovo, A. L.; Calabrese, J. C.; Milstein, D. *J. Am. Chem. Soc.* **1988**, *110*, 6738−6744. (b) Aresta, M.; Quaranta, E.; Dibenedetto, A.; Giannoccaro, P.; Tommasi, I.; Lanfranchi, M.; Tiripicchio, A. *Organometallics* **1997**, *16*, 834−841. (c) Huang, Z.; Zhou, J.; Hartwig, J. F. *J. Am. Chem. Soc.* **2010**, *132*, 11458−11460. (d) Hyster, T. K.; Rovis, T. *J. Am. Chem. Soc.* **2010**, *132*, 10565−10569. (e) Khaskin, E.; Iron, M. A.; Shimon, L. J. W.; Zhang, J.; Milstein, D. *J. Am. Chem. Soc.* **2010**, *132*, 8542−8543. (f) Feller, M.; Diskin-Posner, Y.; Shimon, L. J. W.; Ben-Ari, E.; Milstein, D. *Organometallics* **2012**, *31*, 4083−4101. (g) Wang, L.; Huang, J.; Peng, S.; Liu, H.; Jiang, X.; Wang, J. *Angew. Chem., Int. Ed.* **2013**, *52*, 1768−1772.

(3) Bohle, D. S.; Chua, Z. *Inorg. Chem.* **2011**, *50*, 3135−3140.

(4) (a) Ye, C.; Gao, H.; Twamley, B.; Shreeve, J. N. M. *New J. Chem.* **2008**, *32*, 317−322. (b) Lobanova, A. A.; Il'yasov, S. G.; Popov, N. I.; Sataev, R. R. *Russ. J. Org. Chem.* **2002**, *38*, 1−6.

(5) Sheldrick, G. *Acta Crystallogr.* **2008**, *A64*, 112−122.

(6) Sheldrick, G. M. *SADABS, TWINABS;* University of Göttingen: Germany, 1996.

(7) (a) Spek, A. *J. Appl. Crystallogr.* **2003**, *36*, 7−13. (b) Spek, A. *Acta Crystallogr.* **2009**, *D65*, 148−155.

(8) Andreev, S. A.; Lebedev, B. A.; Tselinskii, I. V. *Zh. Org. Khim.* **1978**, *14*, 2513−2516.

(9) (a) Thiele, J.; Dent, F. *Liebigs Ann.* **1898**, *302*, 245. (b) White, E. H.; Chen, M. C.; Dolak, L. A. *J. Org. Chem.* **1966**, *31*, 3038−3046.

(10) Luk'yanov, O. A.; Kozlova, I. K.; Shitov, O. P.; Konnova, Y. Y.; Kalinina, I. V.; Tartakovsky, Y. A. *Russ. Chem. Bull.* **1996**, *45*, 863−867.

(11) Gattow, G.; Knoth, W. K. *Z. Anorg. Allg. Chem.* **1983**, *499*, 194−204.

(12) Haussler, A.; Klapotke, T. M.; Piotrowski, H. *Z. Naturforsch., B: Chem. Sci.* **2002**, *57*, 151−156.

(13) (a) Lamberton, A. H.; Sutherland, I. O.; Thorpe, J. E.; Yusuf, H. M. *J. Chem. Soc. (B)* **1968**, 6−8. (b) Hampson, P.; Mathias, A. *Chem. Commun.* **1968**, 825−826. (c) Farminer, A. R.; Webb, G. A. *Tetrahedron* **1975**, *31*, 1521−1526.

(14) Coombes, R. G. Nitro and Nitroso Compounds. In *Comprehensive Organic Chemistry;* Pergamon: Oxford, U.K., 1979; pp 305381.
(15) Socrates, G. *Infrared and Raman Characteristic Group Frequencies: Tables and Charts,* 3rd ed.; John Wiley & Sons: Hoboken, NJ, 2004; p 366 pp.
(16) Suchkova, G. G.; Maklakov, L. I. *Vib. Spectrosc.* **2009**, *51*, 333−339.
(17) Nakamoto, K., Part B: Applications in Organometallic Chemistry. In *Infrared and Raman Spectra of Inorganic and Coordination Compounds;* John Wiley & Sons, Inc.: Hoboken, NJ, 2008; p 292.
(18) Deeming, A. J.; Shaw, B. L. *J. Chem. Soc. A: Inorg, Phys, Theor.* **1969**, 1802−1804.
(19) Singer, H.; Wilkinson, G. *J. Chem. Soc. A: Inorg, Phys, Theor.* **1968**, 2516−2520.
(20) Tobe, M. L. B. J. *Inorganic reaction mechanisms;* Longman: Harlow, Essex, England; New York, 1999.
(21) Smith, S. A.; Blake, D. M.; Kubota, M. *Inorg. Chem.* **1972**, *11*, 660−662.
(22) (a) Ruiz, J.; Cutillas, N.; Rodriguez, V.; Sampedro, J.; Lopez, G.; A. Chaloner, P.; B. Hitchcock, P. *J. Chem. Soc., Dalton Trans.* **1999**, 2939−2946. (b) Tellers, D. M.; Ritter, J. C. M.; Bergman, R. G. *Inorg. Chem.* **1999**, *38*, 4810−4818.
(23) Blake, D. M.; Kubota, M. *J. Am. Chem. Soc.* **1970**, *92*, 2578−2579.
(24) Vaska, L. *J. Am. Chem. Soc.* **1966**, *88*, 4100−4101.
(25) La Monica, G.; Cenini, S.; Forni, E.; Manassero, M.; Albano, V. G. *J. Organomet. Chem.* **1976**, *112*, 297−308.